

International Conference on Space Optics—ICSO 2008

Toulouse, France

14–17 October 2008

Edited by Josiane Costeraste, Errico Armandillo, and Nikos Karafolas



Demonstrating improved fibre coupling efficiency by loss-less shaping of top-hat receive beams

Ch. Voland

Y. Tissot

Th. Weigel

Th. Dreischer

et al.

DEMONSTRATING IMPROVED FIBRE COUPLING EFFICIENCY BY LOSS-LESS SHAPING OF TOP-HAT RECEIVE BEAMS

Voland, Ch.⁽¹⁾, Tissot, Y.⁽¹⁾, Weigel, Th.⁽¹⁾, Dreischer, Th.⁽¹⁾, Wallner, O.⁽²⁾, Ergenzinger, K.⁽²⁾,
Ries, H.⁽³⁾, Jetter, R.⁽³⁾, Vosteen, L.L.A.⁽⁴⁾, Barros, J.⁽⁴⁾

⁽¹⁾Oerlikon Space AG, Schaffhauserstr. 580, 8052 Zürich, Switzerland, Email: christoph.voland@oerlikon.com

⁽²⁾EADS Astrium GmbH, Claude-Dornier-Straße, 88090 Immenstaad, Germany,
Email: oswald.wallner@astrium.eads.net

⁽³⁾OEC AG, Lindwurmstrasse 41, 80337 München, Germany, Email: harald.ries@oec.net

⁽⁴⁾TNO Science and Industry, Stieltjesweg 1, 2600 AD Delft, The Netherlands, Email: amir.vosteen@tno.nl

ABSTRACT

The investigations presented below were originally planned on the background of the DARWIN mission. The demand for improved fibre coupling efficiency yet is a general one for applications that cannot cope with the 20% loss of power upon coupling into a fibre. By shaping the transverse amplitude and phase distributions of the receive beam, the single-mode fibre coupling efficiency can potentially be increased to almost 100% (if the beam shaping is lossless), thus allowing for a gain of more than 20% (or 1.07dB) compared to conventional designs.

We show that the use of "tailored freeform surfaces" for purpose of beam shaping reduces the mode mismatch between the Airy pattern of the image and the fibre mode, and therefore allows for achieving a performance close to the physical limitations.

As a follow-up to a previously published paper, [1], we present the design and the results of a proof of concept demonstrator (POCD) for the application of tailored surfaces for building a beam shaping optics that shall enhance fibre coupling performance.

The demonstrator consists of two main parts, the input beam support equipment and the POCD core. The first part contains the laser source, the top hat beam generation optics and a deformable mirror. The POCD core is set up as a three mirror system focussing into the fibre with 1064 nm being the design wavelength.

The experiments performed with the demonstrator aimed at the principle proof of the beam shaping approach and at the test of deviations from the nominal parameters like field angle and aberrations. The results acquired from the experiments with a proof of concept demonstrator in an "as built" configuration show good agreement with the theoretical performance predictions by wave-optical simulations. Limitations of the available manufacturing technologies and of the operating wavelength regime are discussed.

1. INTRODUCTION

The DARWIN mission [2] will search for "earth-like" planets in the vicinity of a central star. This means finding a weak scattering and small object near to a very bright light source. In order to cope with the contrast between the star and the planet a nulling interferometer is set up that shall cancel out the starlight by destructive interference of the receive beams. For improving the performance of interferometer the superimposed beams are coupled into an optical single mode fibre which acts as a modal filter.

Two major challenges result from the DARWIN scenario:

- a nulling ratio of better than $1.5 \cdot 10^{-5}$ [3] which requires an optical instrument design with utmost efficiency to cope with extremely low planet signal levels
- broadband operation over the wavelength range from $4\mu\text{m}$ to $20\mu\text{m}$

2. FIBRE COUPLING ASPECTS

The efficiency of coupling light into a single-mode fibre strongly depends on the matching between the incident diffraction pattern and the principal mode of the fibre, see Fig. 1. A collimated circular beam of a top-hat intensity profile conventionally focussed on the fibre tip forms an Airy pattern which differs from the propagation function of the fibre, the fibre mode, and the coupling efficiency CE (η) cannot be better than 78%.

That maximum of 78% is reached only at the cut-off frequency of the fibre, which corresponds to the shortest wavelength λ_c for single mode operation. The coupling efficiency drops, with increasing slope, at higher wavelengths. (red curve in Fig. 2)

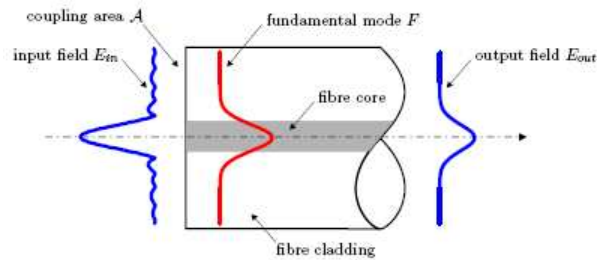


Fig 1. The coupling scenario

By tuning the coupling parameters, and at costs of the maximum achievable CE, the wavelength sensitivity of the curve CE versus λ may be reduced such that at least over one octave $\lambda_c-2\lambda_c$ one obtains a flat and almost constant curve. That is illustrated in Fig. 2. That figure plots the normalised CE versus the normalised frequency. Normalised CE meaning 1.0 equals 78%.

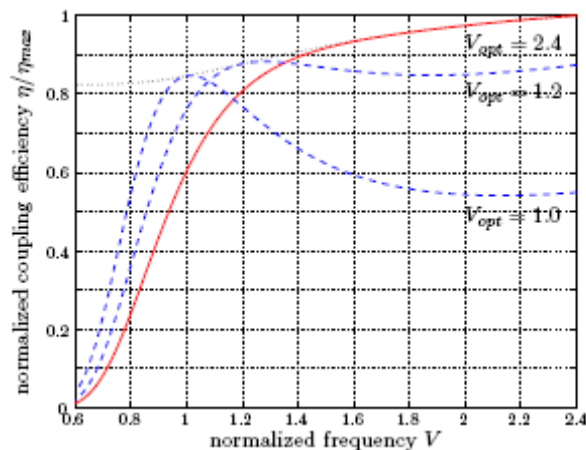


Fig. 2. Drop of the CE versus decreasing frequency V i.e. increasing wavelength λ , for 3 focal lengths.

The normalised frequency V is proportional to the inverse λ :

$$V = \frac{2\pi}{\lambda} r_k \sqrt{n_{co}^2 - n_{cl}^2} \quad (1)$$

where r_k is the core radius and n_{co} , n_{cl} are the refractive indices of core and cladding, All of them are system constants¹, and V varies only with $1/\lambda$ for a given fibre.

A frequency of 2.405 is the cut-off-frequency, the limit of single mode regime. For maximum CE, η_{max} , the focal length of the focussing optics would be tuned such that the diffraction Airy has the best match to the

fibre mode at a λ corresponding to $V=2.4$. That is done in almost all practical applications. The red curve $V_{opt}=2.4$ shows the spectral behaviour. If the focal length is tuned such that the best match results at $2\lambda_c$, (dotted blue curve $V_{opt}=1.2$), the CE is sub-optimal at shorter wavelengths. Within λ_c and $2\lambda_c$, η varies only little between 0.84 and 0.89.

3. FIBRE COUPLING WITH IMPROVED EFFICIENCY

As mentioned above, there is a potential gain of 20% in CE if the mode mismatch can be resolved. This means that the uniform intensity of the incoming beam has to be transformed into an intensity distribution that matches the back-propagated fibre mode. This beam shaping must not affect the other properties of light, i.e. wave front error and polarisation.

3.1 Optical design aspects

The optical design has to provide two main functions, beam shaping and fibre coupling. In order to be prepared for operation in the DARWIN wavelength range, all optical surfaces shall be reflective to prevent from spectral dispersion. The spectral range for the breadboard was defined from 633 nm to 1550 nm in order to have suitable fibres available which can be implemented in a proof of concept demonstrator. The design wavelength is 1064nm.

The intensity redistribution is performed by means of tailored free form surfaces. The approach was developed by the company OEC in Munich [4]. One surface also alters the optical path difference. Thus a second free form surface is needed to correct for the wave front error of the first surface.

The two beam shaping surfaces (Beam Shaping Optics, BSO) receive and provide a collimated beam. A third parabolic mirror delivers the beam to a focus on the fibre tip (Fibre Coupling Optics, FCO) (Fig. 3).

Additionally the reflections of the BSO mirror set fold the beam in two orthogonal planes in order to minimise polarisation degradation. For the same reason, the third mirror, which focuses the light onto the fibre tip, may be substituted by a refractive focusing optics if the application allows for the possible dispersion and transmission.

¹ We may ignore dispersion $n=f(\lambda)$ here, as this affects both n_{co} and n_{cl} , and the difference varies much slower.

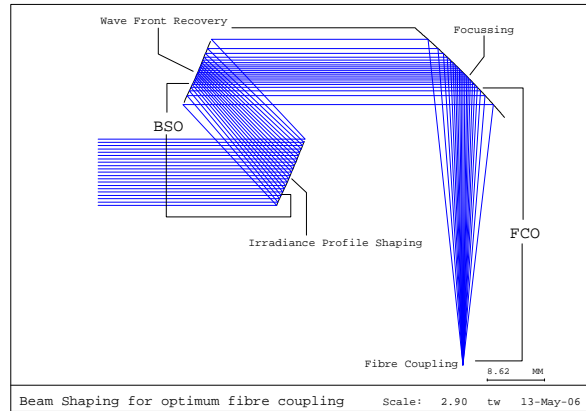


Fig. 3. Optical Design of Beam Shaping (BSO) and Fibre Coupling Optics (FCO).

Fig. 3 visualises the beam shaping effect: the first mirror receives a beam of equal ray density, which changes into a density profile with concentration in the middle.

By increasing the beam size by three times on the secondary mirror and the parabola, the outer part of the fibre mode can also be used.. Theoretically, this design reaches a maximum coupling efficiency of 95%. (100% CE can only be achieved for an infinite large coupling mirror)

The optical design is based on the parameters of the fibre: an OFS Clearlite 630-11 with a cut-off wavelength of 580 nm. The nominal wavelength of operation would be 633 nm.

The focal length (68 mm) is adjusted such that the best coupling efficiency is reached at 1064 nm ($V_{opt}=1.27$, see Fig. 2). Experimental operation was foreseen at laser lines of 633, 1064 and 1300 nm plus also incoherent "white" light.

Further design evolution may eliminate the third mirror and combine the wave front recovery and the imaging function together in one single mirror.

3.2 Simulation

3.2.1 Implementation

For performance analysis the tailored surfaces are implemented to optical design software CodeV via NURBS representation and a user defined interface or ASAP via conversion to Rational Bicubic Splines. Additionally the ESA proprietary software "beam warrior" was used to simulate the full interferometer performance of DARWIN.

The rays can be traced as in any conventional optical system. For purpose of coupling efficiency analysis, the last step from the last parabolic mirror to the image needs the diffractive beam propagator.

3.2.2 Sensitivity and tolerances

The simulations investigated the sensitivity of the optical set-up to misalignments and surface shape errors. The tolerances result in more stringent requirements compared to conventional optics. Concerning the practical purpose of Darwin, the operation wavelengths are longer by a factor of at least 7, and the tolerances scale up accordingly.

Tolerance	Limit
Tilts	< 6 μ rad
Shifts	< 0.3 μ m
Surface figure (WFE_{RMS})	< 3.2 nm

Table 1: Alignment and stability tolerances, $\lambda=1064$ nm

The simulation results show that beam shaping improves the fibre coupling efficiency significantly to the cost of the alignment and manufacturing tolerances. For the proof-of-concept demonstrator the requirements are challenging but feasible

- if the most recently available on the edge manufacturing technologies are applied and
- if the mechanical design provides sufficiently accurate and stable means for adjustment

3.2.3 Spectral performance

The simulations also verified whether the beam shaping would change the spectral behaviour provided in Fig. 2. Normally, both the Airy radius and the fibre mode field diameter increase with the wavelength. The beam shaping is made geometrically and does not scale with the wavelength. The mode matching was designed for 1064 nm.

In fact, Fig. 2 could be reproduced for the normalised effects of the beam shaping with CodeV as shown in Fig. 4. The graphs from Fig. 2 correspond to the dotted lines in Fig. 4, i.e. without the beam shaping. The effect of the beam shaping is shown with the solid lines, which are all above the dotted lines. For the beam shaping optics, this means both the focal length and the beam shaping are optimized for this specific wavelength. In the simulation, only the wavelength changes, the fibre remains the same with $V=2.4$ at 580 nm.

The blue curve for $V_{opt}=1.2$ is almost flat between $V=1.2$ and $V=1.4$. As can be seen from Fig. 4, the degradation of $V_{opt}=1.2$ in comparison to the ideal $V=2.4$ is identical to the non-shaped system, i.e. the blue solid and dotted curves reach the same value for $V=2.4$. At all longer wavelengths towards the left the solid curve is always above the dotted. Thus there is even a relative improvement compared to the non-shaped system. For later experimental verification the curves of Fig. 4 were converted into the absolute coupling efficiency

curves in Fig.5. The absolute improvements by beam shaping become obvious: The distance between the dotted (no BS) and the solid (with BS) lines of one color means the gain in coupling efficiency that can be achieved by beam shaping.

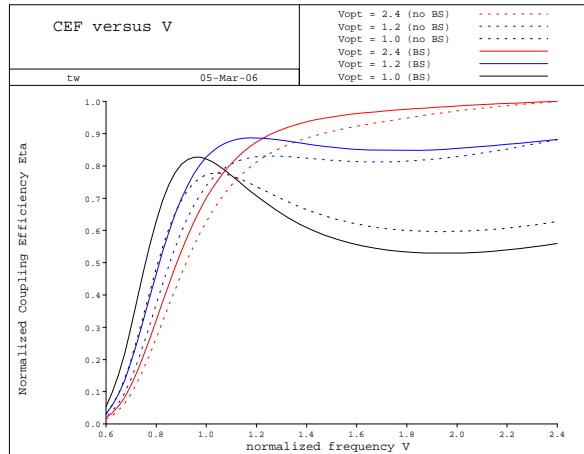


Fig. 4: Spectral behaviour of *normalized* coupling efficiency. $V=2.4$ is 580 nm, $V=1.2$ is 1160 nm.

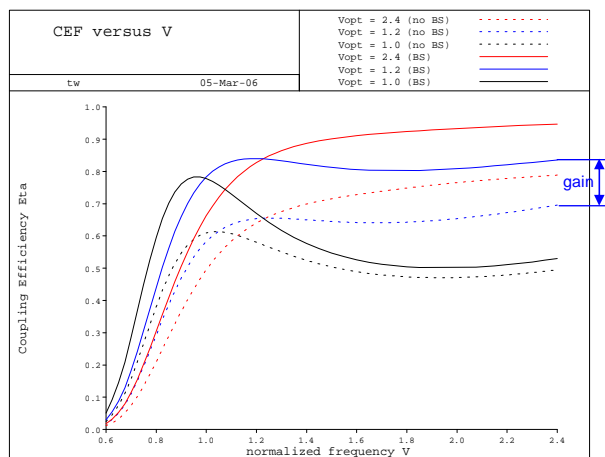


Fig. 5: Spectral behaviour of *absolute* coupling efficiency.

4. EVALUATION

In order to verify the theoretical findings, a demonstrator was built and a verification programme was set up to evaluate the achievable gain in coupling efficiency, the wavelength sensitivity, the impact of aberrations of the input wavefront

4.1 Opto-mechanical design of the demonstrator

The POCD consists of four sections (Fig. 12) of three building blocks:

I. Input beam support equipment:

- Generation of a collimated beam of top-hat intensity

- Introducing / Correction of wave front errors
- The input beam support equipment is provided by TNO (Delft, The Netherlands) made from standard components except for the wave front controlling deformable mirror (DM).

II. The POCD core:

- IIa: Beam shaping
- IIb: Fibre coupling

The POCD core's mechanical design is shown in Fig. 13. The beam shaping optics (BSO) sub-assembly can easily be exchanged by a folding mirror set-up, the non-beam shaping optics (non-BSO), which defines the nominal conditions without beam shaping, see Fig. 14. The mechanical design of the mirrors is the same for any mirror except for the optical surface. Several alignment supporting elements are implemented.

After trading-off several design options, requirements and design drivers with respect to alignment and manufacturing tolerances, polarisation effects and mirror sizes and other aspects, a three mirror design in a three-dimensional configuration was selected, see Fig. 6.

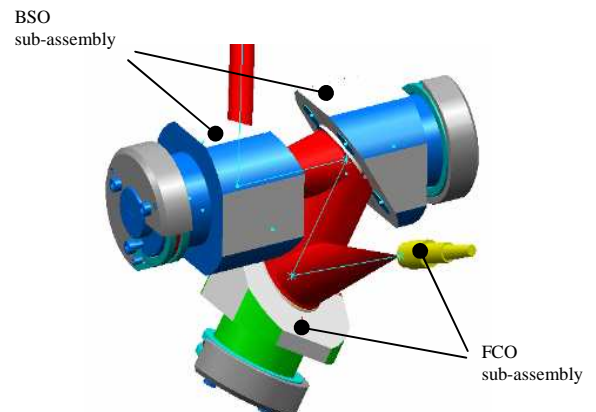


Fig. 6. Opto-mechanical set-up of the beam shaping and fibre coupling optics

III. Detection of the optical output power at the fibre end:

Standard optical powermeters were used for the measurement of the optical power to calculate the power coupling efficiency.

4.2 MAIT

The MAIT process had to face challenges in each discipline:

- **Manufacturing:** The surface figure and the required precision of free form surfaces require on-the-edge technology, in particular because the demonstrator should work at 1064nm nominal wavelength. Diamond tooling by raster fly cutting was selected for the ability to manufacture the optical surfaces, and the opto-

mechanical references of the parts in one run on the same machine. The processing of the optical surfaces was optimised for speed (to avoid long term drifts) and accuracy. The diamond tooling was provided by the LFM (Laboratory for precision machining) in Bremen, [5]

- Assembly and Integration: The three-dimensional set-up requires 5 elements to be adjusted (two beam shaping mirrors, the focusing mirror, the fibre tip), resulting in 26 degrees of freedom. After coarse alignment with the help of the mechanical reference elements, the two sets of two mirrors (non-BSO and BSO) were interferometrically assisted optically adjusted before integration into the POCD core allowed adjustment by optimising the coupling efficiency.

- Testing: For component level tests of the BSO mirrors, there was no calibrated high resolution measurement technique available which could cope with the local slopes and height range. The BSO mirrors could only be tested by interferometry as an assembled set, see Fig 7. The wavefront quality achieved the expected performance.

The intensity redistribution was measured by feeding the POCD core reversely with light out of the fibre. As the fibre generates an ideal fibre mode intensity distribution the beam exiting the POCD core should then show a top-hat profile. This could be verified by beam profiler measurements, see Fig 8.

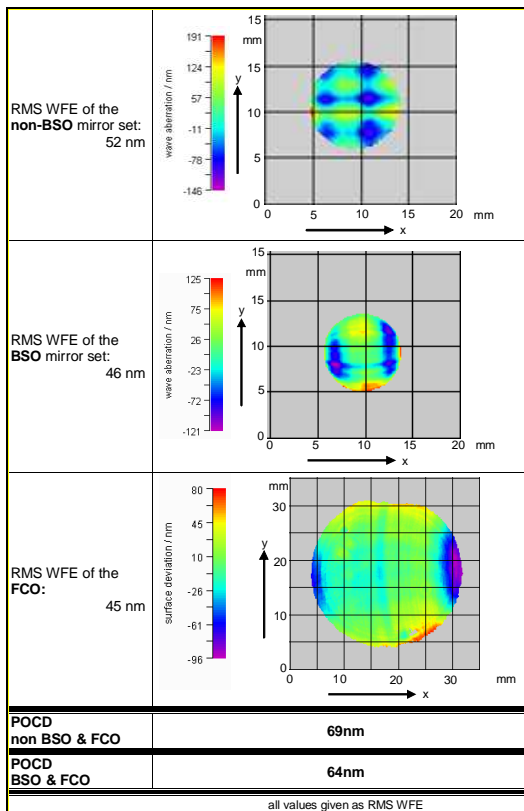


Fig. 7 Wavefront error measurement results and RSS assessment of the POCD core wavefront error

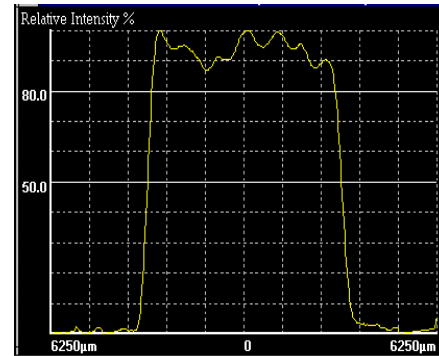


Fig. 8 Intensity profile at the output of the reversely used BSO

The above measurements prove that beam shaping works in theory and in the real life: The intended intensity redistribution was achieved and the wavefront could be maintained as good as the BSO were flat mirrors.

From test results on component level, the performance of the POCD was predicted in order to verify that the later verification programme would give meaningful results. The simulations based on the as-is components showed that the BSO's CE should be $55\% \pm 5\%$ and the non-BSO giving $42\% \pm 5\%$ leaving a minimum difference of 3% between the measurements with both systems at the design wavelength of 1064 nm.

4.3 Verification programme

The verification programme assessed the impacts of various parameters on the performance, i.e. on fibre coupling efficiency in the first degree. The introduced variations were optical aberrations and field angle. Originally the programme intended to test for effects of polarisation, wavelength, and central obscuration on power coupling efficiency, complex coupling efficiency and nulling performance. For reasons of the required resolution of introduced changes and the achievable performance of the POCD build from the "as-is" components in order to get meaningful measurements, the verification programme was reduced to basically test the beam shaping performances.

It should be noted that the spectral transmission of the selected fibre did not allow for tests at longer wavelengths as 1064nm. The simulations could not take into account the spectral material properties of the fibre because they are not public.

The measurements of the set-up with beam shaping optics will be compared to those of the set-up with two folding mirrors which replace the beam shaping surfaces.

4.4 Verification test results

4.4.1 Power coupling efficiency

The power coupling efficiency values which result from the predictions and from the measurements with the POCD are compared in Table 2. The measured coupling efficiency of both POCD versions, with and without beam shaping, range well above the expectations including all losses like fibre transmission, back-reflection at the fibre tip, etc.

PCE	BSO	Non-BSO
Expected, no losses	72%	56%
Expected with losses, best alignment	60%	47%
Measured	62.6%	49.6%

Table 2 Power coupling efficiency predictions and measurements

PCE RATIO	PCE BSO divided by PCE non-BSO
Ideal, no losses	(100% / 78%) = +1.07 dB
Expected, no losses	(72% / 56%) = +1.09 dB
Expected with losses, best alignment	(60% / 47%) = +1.06 dB
Measured	(62.6% / 49.6%) = +1.0 dB

Table 3 Comparison of the fibre coupling gain

The comparison between the measured coupling efficiencies shows the gain provided by the beam shaping to range at approximately 1dB which could be verified despite the limitations of experiment (residual misalignments, losses, etc.).

4.4.2 Impact of aberrations

After having set up the deformable mirror (DM) to deliver a flat wavefront to the entrance of the beam shaping optics, the deformable mirror was operated to introduce additional wavefront aberrations in their definition as Zernike coefficients. Each Zernike coefficient up to the 11th was generated individually with an amplitude of up to 2 rad. The resulting measured coupling efficiency curves are displayed in Fig. 9 and Fig. 10

For both versions of the POCD the curves reach their maximum with an offset for one type of aberration. This points to the main residual misalignment/surface figure error of the assembled and integrated POCD.

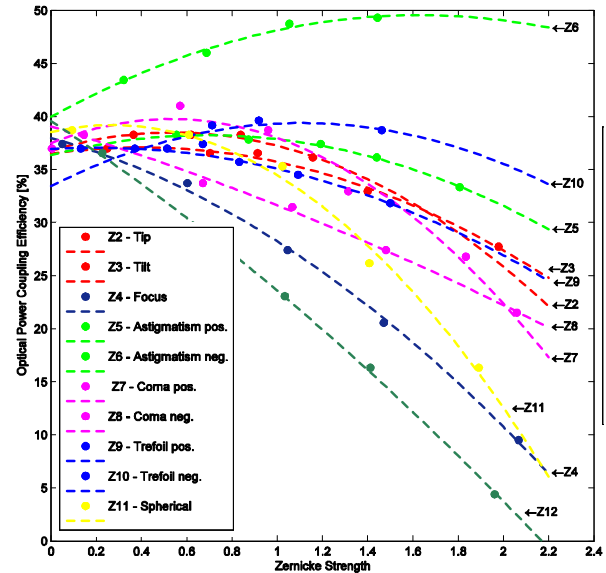


Fig. 9 Coupling efficiency depending on type and strength of aberrations, without BSO

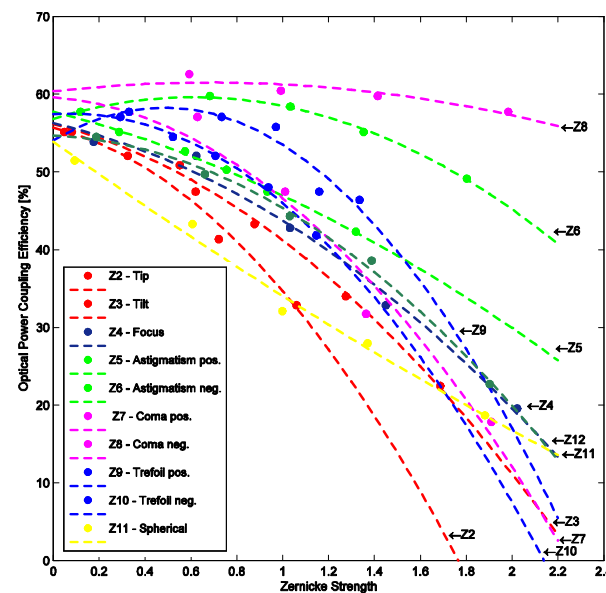


Fig. 10 Coupling efficiency depending on type and strength of aberrations, with BSO

4.4.3 Impact of tilt of the input beam

In particular for DARWIN the sensitivity of the receive optics to tilts of the input beam within the field of view is of special importance because the light of the planet will come at a different angle of incident as the light of the star. This angular separation cannot be resolved the receiving telescope(s). Therefore the enhanced coupling efficiency shall be available for the planet's light. As stated above the improved coupling efficiency by beam shaping is on cost of the sensitivity to deviations from the design parameters, here deviations from the

on-axis beam at zero field angle. For the POCD the coupling efficiency with beam shaping shall remain higher than the CE without beam shaping up to an angle of incidence of 80 microrad in order to cover the DARWIN requirements. Fig. 11 shows the results of the beam warrior simulations (dashed curves) in comparison to the measured values (solid curves) where systematic biases have been removed. Again, the simulations could be verified by the experiment.

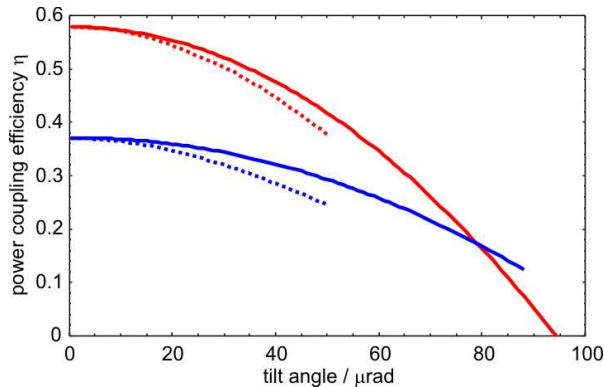


Fig. 11 Gain in CE of the BSO (red) against the unshaped beam (blue); solid lines are the approximations to the measurements, dashed lines are the Beam Warrior simulations

5. CONCLUSIONS

The measurements performed with the Proof-Of-Concept Demonstrator proved the concept of beam shaping for improved coupling efficiency.

The measured gain in coupling efficiency of 1.0 dB is close to the theoretical limit of 1.09 dB.

The optical simulations are in good agreement with the measurements.

On-the-edge manufacturing technology of today allows for figuring optical free form surfaces for applications at wavelength greater and equal 1064 nm.

6. ACKNOWLEDGEMENTS

The work presented above is performed in the frame of the ESA project "Fibre Optic Wave front Filtering" (FOWF) (ESA contract no. 18773/04/NL/HE). We like to thank ESA and their technical officer, Mr. J. M. Perdigues-Armengol for supporting this activity. For their contribution in hardware we thank the LFM (Laboratory for Precision Machining) and their project manager, Mr. K. Rickens.

7. REFERENCES

- [1] Voland, Ch., Weigel, Th., Dreischer, Th., Wallner, O., Ergenzinger, K., Ries, H., Jetter, R., Vosteen, A.: Improving the Fiber Coupling Efficiency for DARWIN by Loss-Less Shaping of the Receive Beams. Proc. of ICSO 2006, Noordwijk, 27. - 30.06.2006
- [2] DARWIN homepage <http://sci.esa.int/science-e/www/area/index.cfm?fareaid=28>
- [3] Darwin, Mission Requirements Document, Sci-A/2005/287/ Darwin/DMS, Issue 1.0, April 2005
- [4] Ries, H, Muschawek J.: Tailored Freeform Optical Surfaces. *JOSA A* Vol. 19 No. 3 March 2002
- [5] Rickens, K.; Riemer, O.; Brinksmeier, E.; Dreischer, Th; Voland, Ch.; Ries, H.: Ultraprecision Manufacturing of Freeform Optical Surfaces for Astronomical Applications. Proc. of EUSPEN, Zürich, 05.2008

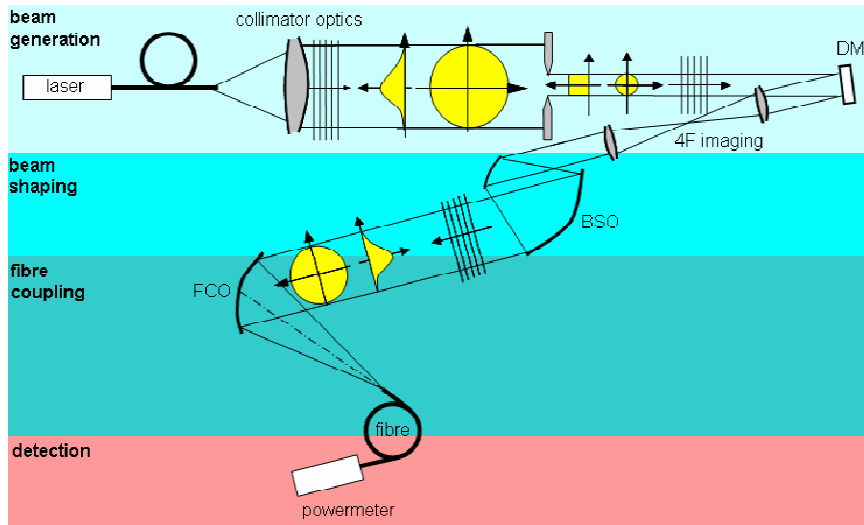


Fig. 12 Proof-Of-Concept Demonstrator scheme

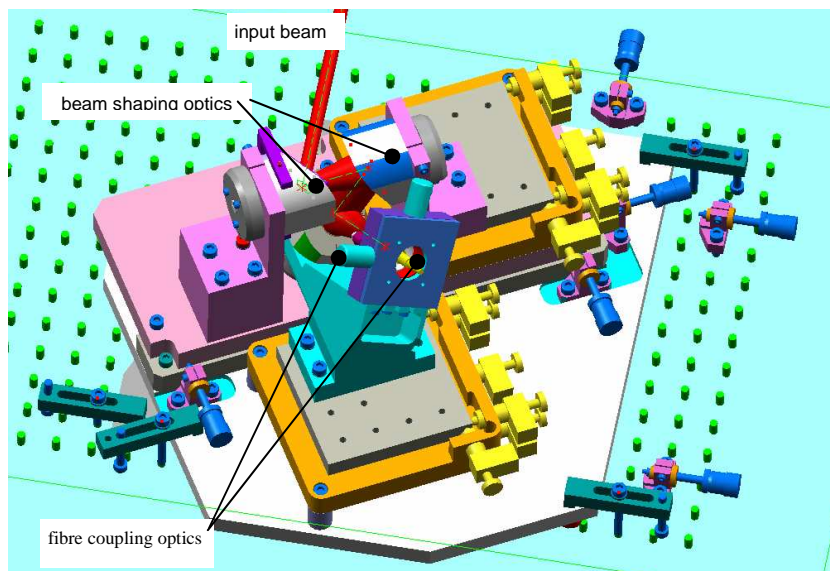


Fig. 13 Mechanical design of the Proof-Of-Concept Demonstrator core

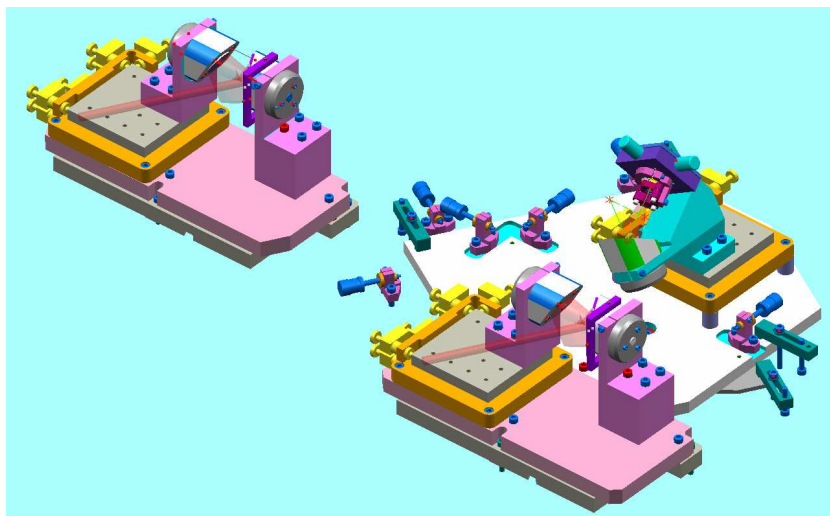


Fig. 14 Exchangeability of non-BSO and BSO